A Smart Frequency Domain-Based Modeling Procedure of Rogowski Coil for Power Systems Applications

Alessandro Mingotti, Lorenzo Peretto, and Roberto Tinarelli
Department of Electric, Electronic and Information Engineering "G.Marconi"
University of Bologna
Bologna, Italy,
alessandro.mingotti2, lorenzo.peretto, roberto.tinarelli3@unibo.it

***Abstract*—Rogowski coils are a key measurement instruments in several applications due to their flexibility, large bandwidth, linearity, etc. Like the majority of the instrument transformers, also Rogowski coils are standardized and their use is regulated almost for every application. This work focuses on a smart way for the equivalent parameters' computation of the Rogowski coil. The parameter computation is performed evaluating the Rogowski response when subjected to a single waveform generated to fulfil a specific requirement on its frequency content. Results demonstrates the equivalency of the presented method compared to the typical frequency sweep test. In addition, the results have been used to validate a Rogowski's output estimate procedure presented by the authors in a previous work.**

Keywords—low-power instrument transformer, impulse response, impedance measurement, frequency domain, Rogowski coil, modelling, power frequency, LPIT, LPCT

I. INTRODUCTION

After the introduction of the IEEE 61869 Standard series [1, 2], the key role of the legacy instrument transformers (ITs) and the new Low-Power Instrument Transformers (LPITs) has been established. As for the former type, their usage in practical applications is consolidated, as well as the related literature, always vivid and up-to-date. In particular, the main fields of LPITs' involvement concern accuracy [3-7], influence quantities [8-11], and modelling [12-14].

Although even ITs still require lot of studies to fully understand their behaviour in several situations, LPITs are a wide-open topic with far more unsolved issues compared to the legacy ones. To this purpose, this paper focuses on LPITs, in particular the passive current type: the Rogowski coil [15]. Both current and voltage LPITs are widely adopted in many Smart Grids application [16-18], as a matter of fact they are more versatile, light, compact, and suitable for all the new arising grid applications. Turning to the Rogowski coils, their use has increased over time due to their flexibility in the installation in uncommon places. In addition, the split-core type makes them suitable for all those a-posteriori applications where the existing network cannot be disconnected to implement a new measurement system. For example, in [19] they have been used in a busbars system, whereas in [20] and [21] an on-site calibration and an application with Phasor Measurement Units (PMUs) have been developed. Moving to the measurement of fast changing currents, impulse currents and short circuit ones have been measured using Rogowski coils in [22] and [23], respectively. Finally, their involvement in Smart Grid applications and their performance evaluation has been studied in [24] and [25, 26], respectively.

Of course, Rogowski coils have also some drawbacks. For example, (i) they are affected by external influence quantities, (ii) they feature high nominal ratios, which result in very low voltage outputs (hence, the noise could be an issue during the measurements), (iii) they are sensitive to transients (by considering the derivative working relation as detailed in the following).

In light of the aforementioned, the research presented in [27], of which this paper represents a technical extension, showed the behaviour of Rogowski coils when used with not-rated burdens (defined in [2]). In addition, [27] provided a simple modelling procedure, based on a frequency characterization, to obtain the equivalent parameters of the coil and to predict its output when used with non-rated burdens.

In this work, a further step is done to simplify the modelling procedure of the Rogowski. In particular, a proper time-domain signal has been used to obtain the above parameters with a "single shot" test. Then, such a single signal has been used to test the 3 Rogowski coils introduced in [27].

Aim of such a test is to obtain the effects of an impulse response test but with a controlled frequency spectrum, as described in the following.

The use of impulses is not new in literature. As a matter of fact, impulses are used in acoustic [28], semiconductors [29], power transformers [30-32], etc. As for ITs, impulse-based techniques are used for their modelling [33, 34], error analysis [35], and for the well-known Frequency Response Analysis (FRA) [36-38] adopted for multifold purposes.

However, to the authors' knowledge the ad-hoc generation of signals for the Rogowski modelling is a topic not tackled in the literature yet. Furthermore, the paper aims at suggesting a single test to obtain an accurate equivalent impedance of the Rogowski within a frequency range that contains the power quality spectrum one (0 - 5 kHz).

From the results, it is possible to appreciate the effectiveness of the method and the equivalency with the typical frequency sweep test.

Finally, the Rogowski's output estimate procedure presented in [27] has been applied, using the new results as input quantities, and compared with experimental measurements. The encouraging results confirm the validity of the presented procedure.

The paper is structured as follows: Section II briefly recalls the working principles of the Rogowski coils, including its modelling. The measurement setup, developed in [27] is summarized in Section III. Section IV describes the performed tests, whereas the measurement results are collected in Section V. The procedure presented in [27] is validate in Section VI. Finally, a conclusion is drawn in Section VII.

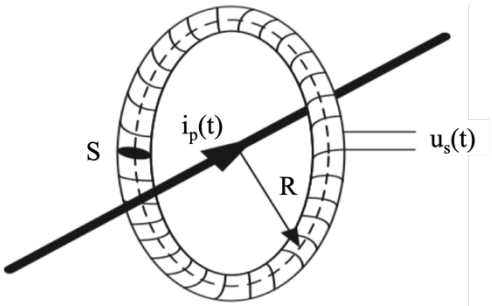

Fig. 1. Working principle schematization of the Rogowski coil

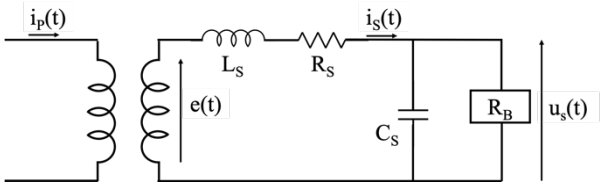

Fig. 2. Circuit diagram of the Rogowski coil equivalent circuit

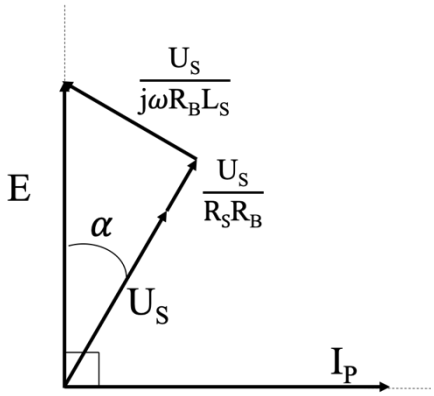

Fig. 3. Phasor diagram of the Rogowski coil equivalent circuit

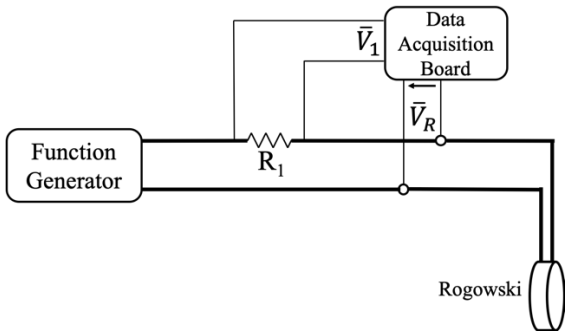

Fig. 4. Equivalent circuit of the characterization setup

II. Rogowski Coil Principles

Besides the existence of several current transducers or LPCTs, this paper focuses and Rogowski coils as described in the Standard IEC 61869-10 [39], hence without the integrating part.

The Rogowski Coil is an instrument transformer which operates according to the Ampere's law. As schematized in Fig. 1, it consists of a coil wounded around an insulating material (air, plastic, etc.). Then, the primary conductor,

TABLE I. Main characteristics of the NI 9238

Architecture	24-bit	**Max input signal**	±500 mV
Sample rate	50 kS/s/ch	**Simultaneous channels**	YES
ADC	Delta Sigma	**Temperature range**	-40 to 70 °C
Gain Error (% of reading)	±0.07 %	**Offset Error (% of range)**	±0.005 %

TABLE II. Main Characteristics of the Rogowski coils under test

Feature	**A**	**B**	**C**
Type	Split-core	Split-core	Split-core
Ratio	1000 A/ 333 mV	1000 A/ 100 mV	1000 A/ 100 mV
Inner Diameter	150 mm	115 mm	75 mm
Accuracy	±1 %	±1 %	±1 %

whose current has to be measured, is placed inside the coil. The relation between the primary current $i_P(t)$ and the output of the Rogowski $u_s(t)$ is:

$$u_s(t) = -M\frac{di_P(t)}{dt}. \quad (1)$$

From (1) it is clear that the output of the instrument transformer is a voltage proportional to the derivate of the primary current and to M, the mutual inductance between the conductors.

As for the model of the Rogowski, it is typically represented by an equivalent circuit as the one in Fig. 2, where L_S, R_S, and C_S are the equivalent inductance, resistance, and straight capacitance of the lumped model, respectively. R_B is the high impedance burden [2], whereas $e(t)$ is the voltage induced by the primary current, according to:

$$\mathrm{E} = \mathrm{j}\omega M I_P, \quad (2)$$

being ω the angular velocity at the current frequency, I_P is the rms value of $i_P(t)$ and E the rms value of $e(t)$. In terms of phasors, the quantities presented with the model are linked to each other as in Fig. 3 (not in scale). From the picture it emerges the 90° shift between the input and the output of the Rogowski, which is slightly affected by an angle α due to the presence of L_S (in Fig. 3 the effect of C_S has been omitted). Furthermore, a phase error contribution is given by the burden capacitance in the case of long connection cables and in high frequency applications.

III. Measurement Setup

The setup developed in [27] and depicted in Fig. 4 is here briefly recalled, highlighting some minor changes. It consists of an Agilent 33250A Function Generator (FG), a 10 kΩ high precision resistor (R_1), a NI Data AcQuisition board 9238, which characteristics are listed in Table I, and of course the 3 Rogowski coils under test (RUT).

The resistor's R_1 combined uncertainty is 0.02 Ω and it has been calculated according to the Guide for the expression of Uncertainty in Measurements [40] using measurements performed with the Digital Multimeter 3458A.

As for the 3 off-the-shelf RUTs, their characteristics are listed in Table II. In accordance with [27] they are referred to as A, B, and C, for the sake of privacy.

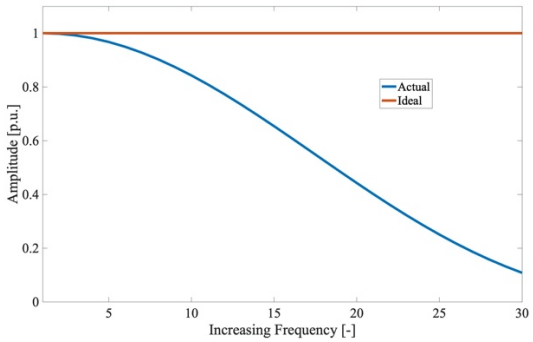

Fig. 5. Actual and ideal amplitude response to an impulse input

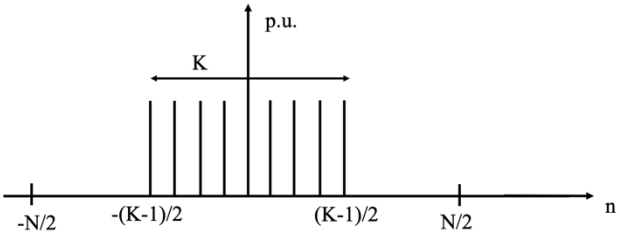

Fig. 6. Generic discrete sequence of N points

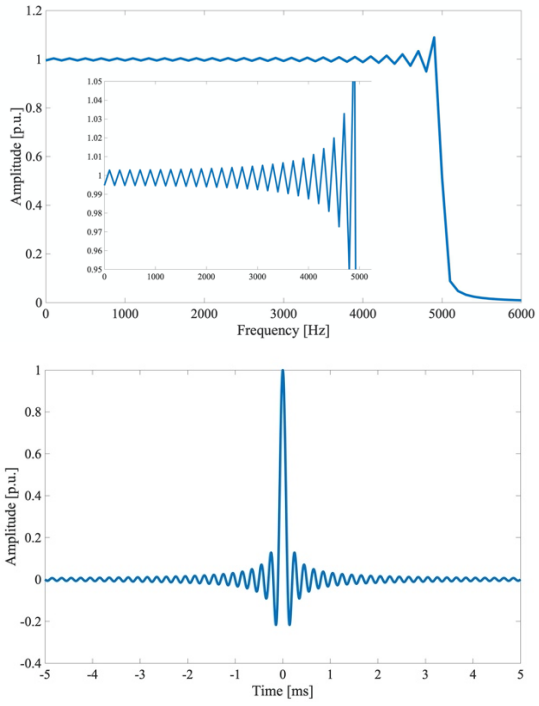

Fig. 7. Signal reproduce with the FG and applied to the RUT. a) frequency-domain; b) time-domain

The operation of the setup consists of feeding the RUTs with the FG and then the voltage and the current (as voltage drop on R_1) affecting the RUTs are collected with the DAQ. In the next Section is described the signal generated for testing the RUTs.

IV. Experimental Tests

A. Signal Generation

The common FRA, for testing linear time-invariant systems, is performed applying impulse signals. Theoretically, the infinite impulse corresponds to a constant signal in the frequency domain; hence, the object under test is stressed with a signal containing all the frequency components from minus to plus infinite. However, as proved and detailed in [41], the finite impulse that a typical generation system can reproduce is far from being ideal. As obvious, the instrumentation allows to reproduce impulses with limited amplitude and not-null duration. Consequently, the frequency response behaviour it will be like the one presented in Fig. 5. In the graph, the ideal and the actual frequency domain impulses are presented. As it can be seen, the amplitude of the frequency components is decreasing as the frequency increase.

Therefore, to tackle such an issue, the desired signal has been generated starting from the frequency domain. In particular, the aim is to have a constant signal for the frequency components up to 5000 Hz and null elsewhere. This choice of having twice the power quality frequency range has been taken to ensure the maximum stability of the input signal up to 2500 Hz. In other words, the aim is to obtain a rectangular window in the frequency domain.

To do this, to the general discrete sequence of Fig. 6 has been applied the following well-known function:

$$h(n) = \frac{\sin(\pi n K/N)}{N \sin(\pi n/N)}, \tag{3}$$

where n is the sequence index, N is the overall number of points and $K$is the number of not-null points of the sequence. In case of $K = N$, (3) can be simplified as:

$$h(n) = \frac{\sin(\pi n)}{N \sin(\pi n/N)}, \tag{4}$$

In Fig. 7a and 7b, are depicted the frequency spectrum of $h(n)$ and its p.u. amplitude, respectively. As for the x axes, they reflect the actual signal injected into the RUTs: a frequency spectrum up to 5 kHz, and a correspondent time signal of period 10 ms to obtain a frequency resolution of 100 Hz. By looking at Fig. 7a and to the zoom included in it, it is possible to highlight the behaviour of the frequency domain signal. It presents oscillations due to the fact that the length of the adopted signal is not infinite but extremely limited over time. Of course, the consequent amplitude variation in the frequency spectrum could have been reduced increasing the time window of the signal depicted in Fig. 7b; with the effect of an higher frequency resolution, not acceptable in this work.

B. Tests Description

In the following, a sweep frequency test and a test applying $h(n)$ are described. Before that, it is necessary to clarify the fact of repeating the sweep test performed in [27]. As a matter of fact, the 4 mA injected in the RUTs is a value that does not reflect the rated value of the current flowing through the secondary terminals of the RUTs. For example, in the case of

RUT A, considering the ratio 1000 A/ 330 mV and the 2 M Ω rated burden, the current flowing in the secondary is around few micro ampere. In light of this, the sweep tests have been repeated to avoid any thermal effect on the coils' impedances

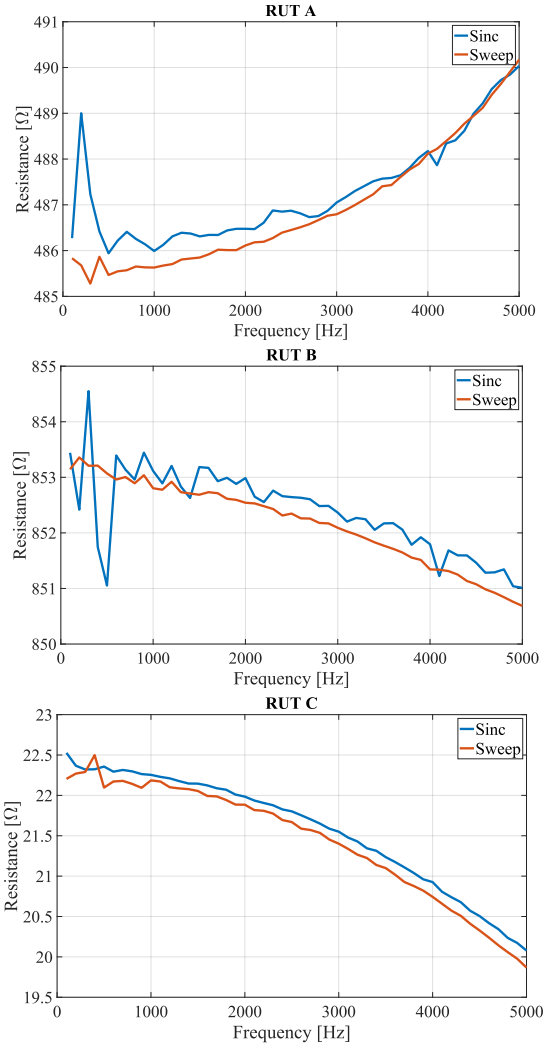

Fig. 8. Resistive part of the Rogowski's impedance for RUT A, B, and C

due to the injected current. In detail, for both the following tests the maximum RMS value of the applied current is 25 μA.

1) Sweep Frequency Test

For the three RUTs, with the FG a sinewave of amplitude 0.4 VPP has been applied to the secondary RUTs' terminals with a frequency step of 100 Hz in the range 0 – 5 kHz. For each frequency, 1 s of measurements for 100 times has been acquired with the DAQ at 50 kS/s. The measurements collected include: the voltage phasors $\bar{V}_R$ and $\bar{V}_1$, that are the voltages at the RUT's terminals and the voltage drop on R_1, respectively. From $\bar{V}_1$, $\bar{V}_R$, and R_1, it is possible to compute the RUT's impedance at each frequency as:

$$\bar{Z}_S = \frac{\bar{V}_R R_1}{\bar{V}_1}, \tag{5}$$

2) "Single shot" Test

Referring to Fig. 4, for the 3 RUTs the following test procedure applies. With the FG the voltage waveform depicted in Fig. 7b) has been continuously applied to the RUT and to the shunt resistor. The period of the $h(n)$ function is 10 ms and the amplitude is 0.4 VPP. Afterwards 500 Sa, corresponding to one period of $h(n)$, have been acquired with the DAQ (at 50 kSa/s) at both the RUT and the shunt

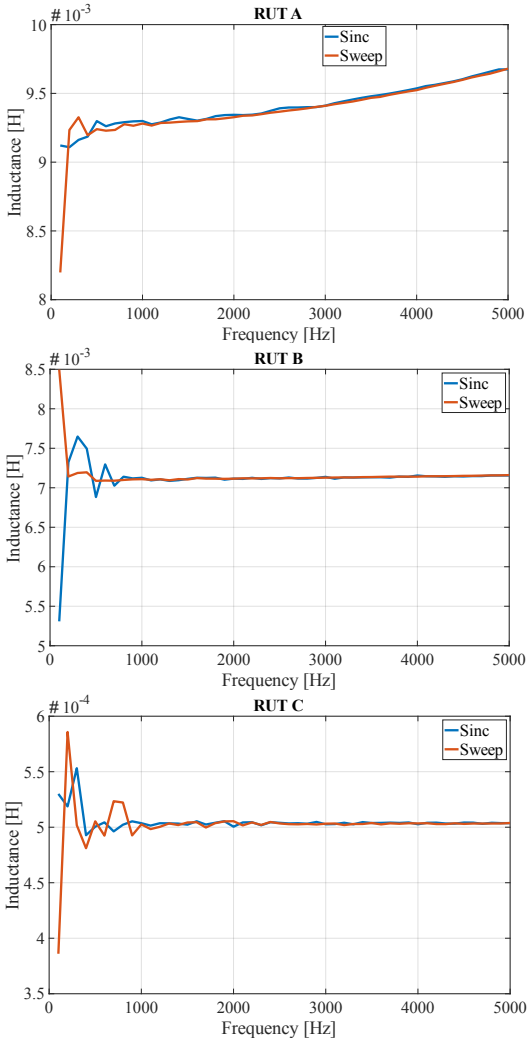

Fig. 9. Rogowski's inductance for RUT A, B, and C

terminals. In this way, the voltage and the current phasors affecting the RUT are completely known. Of course, the current has been obtained from the voltage drop on R_1. Such procedure has been then repeated, for each RUT, 100 times, analogously to what done for the sweep test.

Afterwards, the Fast Fourier Transform (FFT) has been applied to $\bar{V}_R$ and to $\bar{V}_1/R_1$ to extract the impedance of the RUT at each frequency component from 100 Hz to 5 kHz.

V. Experimental Results

Fig. 8, and 9 show all the obtained results. In particular, Fig. 8 contains the resistive part of the impedances for RUTs A, B, and C, from the top to the bottom, respectively. In the graph, both the sweep frequency and the "single shot" tests are depicted. With the same criteria, the computed inductive part of the RUTs' impedances is presented in Fig. 9.

For both the resistance and the inductance, the frequency resolution of the graphs is 100 Hz.

A first general comment on both figures is the evident superimposable behaviour of the impedance computed in the two presented ways. Consequentially, it is possible to save a lot of testing time for the frequency characterization of the devices. In particular, considering (i) 10 ms duration for both the "single shot" test and a single measurement of the frequency sweep test, (ii) 100 measurements for each frequency, the overall test time is 1 s and 50 s for the "single shot" test and the frequency sweep test, respectively. A duration 50 times greater may be not significant in a research laboratory environment, but could become a huge money saving for testing processes inside industries.

A second general comment on Fig. 9 is the flatness of the inductance value over frequency. For the 3 RUTs, considering the scale adopted, the variation of the inductance is limited. Quantifying, for all RUTs, and for both test methodology the maximum variation in the power quality frequency range is less than 10 %. The same content can be extended to the resistances, for all cases. However, the inductance variation is less significant in the overall due to its limited contribution to the RUT impedance.

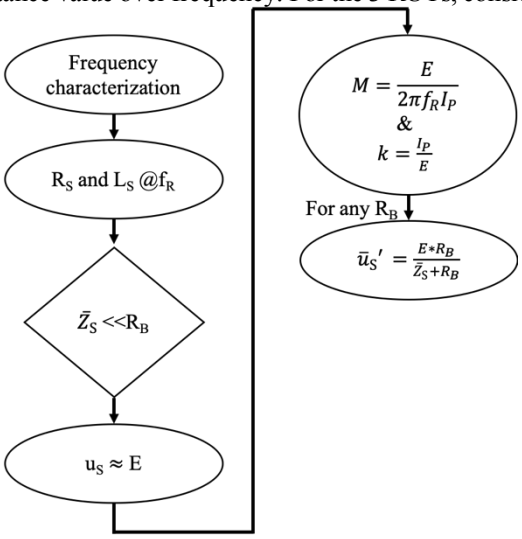

Fig. 10. Flowchart of the Rogowski modelling procedure.

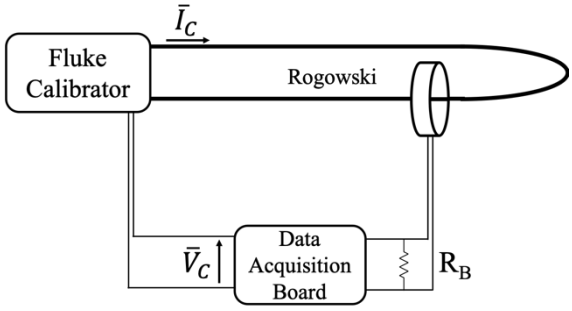

Fig. 11. Equivalent circuit of the validation test setup.

TABLE III. COMPARISON BETWEEN THE ESTIMATE AND THE MEASURED SECONDARY VOLTAGE OF THE THREE RUTS

Device	u_{est} [V]	u_{exp} [V]
RUT A	0.07622	0.07629
RUT B	0.02066	0.02071
RUT C	0.02144	0.02146

As a final general comment, it is possible to appreciate in almost all graphs of Fig. 8 and 9 an initial oscillation of the quantities. This phenomenon may be attributed to three contributes:

- Amplitude of the test signals. Even if the two type of tests share the 0.4 V_{PP}, due to the sinc shape the amplitude of the frequency components are 10 times lower than those of the sweep test;
- Amplitude of the secondary lobes. The amplitude of the external lobes is fraction of millivolt, hence the contribution of the noise becomes significance during the acquisition of the signal;
- Main lobe of the sinc. Its duration is double the one of the secondary lobes, but the number of samples that describe it are the same for all lobes. Therefore, in light of the small amplitudes involved on the voltage, the presence of noise and disturbances affects the quality of the main lobe samples which turns into a distortion of the low frequency components of the signal. This effect may be reduced by increasing the sampling frequency even if it should be considered that its numerical impact is very low, in the order of 1/1000.

Turning to the resistance values, the behaviour of the RUT A is opposite compared to the other two devices. This may be attributed to a still too high current flowing through the secondary terminals. As a matter of fact, the curve resembles the typical behaviour of a conductor that is being heated up by the current during the test. Looking instead to the behaviour of RUT B and C in Fig. 8, a preliminary explanation can be provided considering that the internal structure (conductor details, insulating materials, ground, etc.) is unknown for the end users and the authors. However, the decreasing of the resistive part of the impedance vs frequency may be attributed to the parasitic parameters. In other words, an increasing frequency creates alternative paths for the current which flows through the parasitic parameters. Therefore, the current interesting the RUT is less than the measured (as in Fig. 4), hence the overall effect is a reduction of the RUT's impedance. The fact that only the resistance is affected by such a reduction may be explained by the capacitive nature of the parasitic parameters – which increase proportionally to the frequency – that compensate the inductance variation.

VI. MODEL VALIDATION

A. Model Recall

Starting from the obtained results, in this section it is demonstrated the validity of the modelling process presented in [27]. It allows to estimate the Rogowski's output when working with not-rated burdens (a typical situation among off-the-shelf products). Such a process is now implemented with the parameters of the RUTs obtained from the "single shot" test described in Section IV. For the sake of clarity, in Fig. 10 is recalled the flowchart of the modelling procedure described in [27]. In brief, the procedure consists of a first frequency characterization, which allows to evaluate the equivalent impedance of the RUT comparing it with the standard burden (2 MΩ). Such an impedance is always far lower than 2 MΩ, hence, for the next step of the model it has been neglected. At the desired operating frequency f_R, the mutual inductance M is computed starting from tests at different input currents and with the rated burden connected to the RUT.

Once M is known, the voltage E (see (2)) can be calculated for whatever combination of input current and frequency (as it has been done for the validation, described in the next subsection). Finally, the voltage output at the RUTs' terminals can be estimated for whatever burden connected to RUT.

B. Validation

The encouraging results obtained in the previous section are here used to validate the model presented in [27]. To this purpose, the setup depicted in Fig. 11 has been used. Briefly, a calibrator Fluke 6105a is used to inject the current $\bar{I}_C$ into the primary of the RUT. Then, the DAQ NI 9238 acquires the secondary voltage of the RUT, which is applied to the generic burden R_B, and the reference signal from the calibrator $\bar{V}_C$, to be used as phase reference for the RUTs.

With such a setup, and two burdens, the rated 2 MΩ and a generic 22 kΩ, two main tests have been performed. The 22 kΩ burden has been selected because in [27] it has been confirmed that it already makes the output of the Rogowski varies, compared to the rated burden. Furthermore, it is high enough to avoid the circulation of any high current through the Rogowski's impedance.

The first test consisted of injecting a sinusoidal current at 50 Hz with an RMS value of 100 A. The second test instead, consisted of injecting a 1000 Hz sinusoidal signal with an amplitude of 10 A (hence 10 % of the previous test). The aim of this second test is to stress the RUTs with a random atypical signal. For all tests, 100 measurement of 10 periods of the main signal have been collected.

Afterwards, the measurements at 2 $M\Omega$ provide the secondary RUTs voltages $\bar{E}_{50}$ and $\bar{E}_{1k}$ (for the 50 Hz and 1 kHz tests, respectively) to be used in the procedure depicted in Fig. 10 and in particular in the last step. This can be rewritten as:

$$\bar{u}_{50} = \frac{\bar{E}_{50} * R_B}{\bar{Z}_{\mathrm{S50}} + R_B} \tag{6}$$

$$\bar{u}_{1k} = \frac{\bar{E}_{1k} * R_B}{\bar{Z}_{\mathrm{S1k}} + R_B} \tag{7}$$

where the complex numbers $\bar{u}_{50}$ and $\bar{u}_{1k}$ are computed with the burden $R_B = 22\ k\Omega$ and the impedances of the RUTs $\bar{Z}_{\mathrm{S50}}$ and $\bar{Z}_{\mathrm{S1k}}$. The first parameter refers to the real and imaginary part of the RUT impedance at 50 Hz, whereas the latter to the impedance at 1 kHz; both obtained with the "single shot" test described in Section IV.

Afterwards, from $\bar{u}_{50}$ and $\bar{u}_{1k}$ to sinewaves have been generated to sum the two contributions obtaining a unique signal. This signal is the estimate of the RUT's secondary voltage with the 22 $k\Omega$ burden.

Finally, the above described measurements performed with the 22 $k\Omega$ burden have been used to assess the estimates computed with the presented method. To this purpose, the time domain signals of the 50 Hz and 1 kHz test have been summed exploiting the superposition principle and the linearity of the Rogowski.

The effectiveness of the presented procedure can be assessed from the values in Table III. It contains the estimate of the secondary voltage of the RUTs, u_{est}, and the measured value u_{exp} (both RMS) obtained from the experimental measurements. The choice of using the RMS as the index for the comparison is due to the limited influence of the inductance compared to the resistance in the Rogowski impedance, hence on the phase. In fact, the reactive part (up to the power quality frequency range) it is typically few percent of the resistive one. The values in Table III have been reported according to the measured standard deviation of the mean (order of 10^{-5}). From them, it is possible to appreciate at a glance the validity and applicability of the procedure described in [27] and above recalled, even in the case of non-rate conditions of the primary current and of the connected burden.

VII. Conclusions

The aim of this work is to describe a different way to perform a frequency characterization in twice the power quality frequency domain applying just a signal. Such a signal has been generated starting from the desired frequency spectrum. The results of the characterization, performed on three different Rogowski, have been compared with the typical frequency sweep test. From the comparison it is possible to appreciate the consistency between the two methodology, hence the applicability of the proposed one. Furthermore, the obtained results have been used to validate an estimation procedure to predict the secondary output a Rogowski coil when fed with distorted waveforms and connected to not-rated burdens. Again, from the results it is confirmed the effectiveness of the estimating procedure and its usability in laboratory or in-field applications.

References

[1] IEC General requirements for instrument transformers, IEC-61869-1, 2016.

[2] IEC Additional requirements for low-power instrument transformers, IEC-61869-6, 2016.

[3] G. Mahesh, B. George, V. Jayashankar, V.J. Kumar, "Instrument transformer performance under distorted-conditions", Proceedings of the IEEE INDICON, India, 2004.

[4] G. Pasini, L. Peretto, P. Roccato, A. Sardi, R. Tinarelli, "Traceability of low-power voltage transformer for medium voltage application", IEEE Transaction on Instrumentation and Measurement, vol. 63, no. 12, pp. 2804-2812, May 2015.

[5] A. Cataliotti, V. Cosentino, et al., "Metrological performances of voltage and current instrument transformers in harmonics measurements", International Instrumentation and Measurement Technology Conference, Houston, USA, July 2018.

[6] K. Draxler, R. Styblikova, "Calibration of instrument current transformers at low currents using lock-in amplifier", International Conference on Applied Electronics, Pilsen, Czech Republic, Oct. 2017.

[7] A Mingotti, L Peretto, R Tinarelli, A Ghaderi, "Uncertainty sources analysis of a calibration system for the accuracy vs. temperature verification of voltage transformers", Journal of Physics: Conference Series 1065 (5), 052041.

[8] M. Paredes-Olguin, C. Gómez-Yáñez, F. P. Espino-Cortés, E. Ramirez, "Electric stress grading on bushings of combined instrument transformers using high permittivity polymeric composites", IEEE Electrical Insulation Conference, Ottawa, Canada, June 2013.

[9] A. Mingotti, G. Pasini, L. Peretto, R. Tinarelli, "Effect of temperature on the accuracy of inductive current transformers", IEEE International Instrumentation and Measurement Technology Conference, Houston, TX, USA, 2018.

[10] Z. Li, Y. Du, A. Abu-Siada, Z. Li, T. Zhang, "A New Online Temperature Compensation Technique for Electronic Instrument Transformers", IEEE Access, vol.7, pp. 97614-97623, July 2019.

[11] A. Mingotti, L. Peretto, R. Tinarelli, F. Mauri, I. Gentilini, "Assessment of Metrological Characteristics of Calibration Systems for Accuracy vs. Temperature Verification of Voltage Transformer", IEEE Workshop on Applied Measurements for Power Systems, Liverpool, UK, Sep. 2017.

[12] J. Jasche, P. Schegner, “A model to compute the resonance effects in high current instrument transformers”, IEEE International Magnetics Conference, Dublin, Ireland, Aug. 2017.

[13] “Electromagnetic Modeling of a High Voltage Current Transformer”, North American Power Symposium, Las Cruces, USA, Dec. 2007.

[14] F. Della Torre, M. Faifer, et. al., “Instrument transformers: A different approach to their modeling”, IEEE Workshop on Applied Measurements for Power Systems, Aachen, Germany, Sep. 2011.

[15] IEC Additional requirements for low-power passive current transformers, IEC-61869-10, 2017.

[16] A. Larrabeiti, Z. Ojinaga, V. Macías, I. Garabieta, J. A. Lozano, M. G. Zamalloa, “Low-power instrument transformer-based MV automation: lessons learned and future applications”, CIRED - Open Access Proceedings Journal, vol. 2017, no. 1, pp. 1291-1294, Oct. 2017.

[17] A. Mingotti, L. Peretto, R. Tinarelli, “Low Power Voltage Transformer Accuracy Class Effects on the Residual Voltage Measurement”, proc of 2017 IEEE “International Instrumentation and Measurement Technology Conference”, I2MTC, May 15-18, 2018.

[18] L. Bartolomei, A. Mingotti, L. Peretto, R. Tinarelli, G. Pasini, L. Puddu, P. Rinaldi, “Performance evaluation of an energy meter for low-voltage system monitoring”, 22nd World Congress of the International Measurement Confederation, Belfast, UK, Sept. 2018.

[19] P. Wang, G. Zhang, X. Zhu, C. Luo, “Planar Rogowski Coil Current Transducer Used for Three-phase Plate-form Busbars”, IEEE Instrumentation & Measurement Technology Conference, Warsaw, Poland, May 2007.

[20] E. P. Suomalainen, J. K. Hallstrom, “Onsite Calibration of a Current Transformer Using a Rogowski Coil”, *IEEE Transactions on Instrumentation and Measurement,* vol. 58, no. 4, pp. 1054-1058, Apr. 2009.

[21] A. Mingotti, L. Peretto, R. Tinarelli, A. Angioni, A. Monti and F. Ponci, “Calibration of Synchronized Measurement System: from the Instrument Transformer to the PMU”, IEEE proc. of “Applied Measurements for Power Systems”, AMPS, Sep. 2018.

[22] W. Limcharoen, P. Yutthagowith, “Rogowski coil with an active integrator for measurement of switching impulse current”, 10th International Conference on Electrical Engineering/Electronics, Computer, Telecommunications and Information Technology, Krabi, Thailand, May 2013.

[23] D. Jarry-Bolduc, B. Djokic, “Hydro-generator sudden short-circuit testing using Rogowski coils”, Conference on Precision Electromagnetic Measurements, Ottawa, Canada, July 2016.

[24] Z. Kołodziejczyk, P. Michalski, W. Kardyś, “Novel autonomous voltage and current measurement unit for Smart Grids”, International Symposium on Power Electronics Power Electronics, Electrical Drives, Automation and Motion, Sorrento, Italy, June 2012.

[25] Z. Z. Sheng, B. Han, M. A. Qing, “The analysis of the factors affecting the performance of Clamp Rogowski coil”, International Conference on Power System Technology, Chengdu, China, Oct. 2014.

[26] M. Chiampi, G. Crotti, A. Morando, “Evaluation of flexible Rogowski coil performance in power frequency applications”, *IEEE Transactions on Instrumentation and Measurement*, vol. 60, no. 3, pp. 854-862, March 2011.

[27] A. Mingotti, L. Peretto, R. Tinarelli, “A Simple Modelling Procedure of Rogowski Coil for Power Systems Applications”, Workshop on Applied Measurements for Power Systems, Aachen, Germany, Sep. 2019.

[28] “Dynamic impulse response model for nonlinear acoustic system and its application to acoustic echo canceller”, IEEE Workshop on Applications of Signal Processing to Audio and Acoustics, New Paltz, USA, Dec. 2009.

[29] S. V. Averine, N. V. Alkeev, “Impulse response of the metal-semiconductor-metal photodetector”, International Conference on Ultrawideband and Ultrashort Impulse Signal, Sevastopol, Ukraine, Dec. 2012.

[30] H. Rahimpour, S. Mitchell, S. Rahimpour, “Online monitoring of power transformers using impulse frequency response analysis”, Iranian Conference on Electrical Engineering, Tehran, Iran, July 2017.

[31] J. J. Wu, J. J. Huang, T. Qian, W. H. Tang, “Study on Nanosecond Impulse Frequency Response for Detecting Transformer Winding Deformation Based on Morlet Wavelet Transform”, International Conference on Power System Technology, Guangzhou, China, Jan. 2019.

[32] V. Premalatha, S.S. Sruthi, M. Vikash, M. K. Ilampoornan,“Instrument transformer winding fault analysis using frequency response analysis”, International Conference on Advanced Communication Control and Computing Technologies, Ramanathapuram, India, Oct. 2012.

[33] A. Elhaffar, M. Lehtonen, “High Frequency Current Transformer Modeling for Traveling Waves Detection”, IEEE Power Engineering Society General Meeting, Tampa, USA, July 2007.

[34] M. Dadic, T. Zupan, G. Kolar, “FIR modeling of voltage instrument transformers from frequency response data”, International Colloquium on Smart Grid Metrology, Split, Croatia, May 2018.

[35] S. Q. Chen, J. M. Li, T. Luo, H. Y. Zhou, Q. X. Ma, L. Du, “Study on the impulse characteristics of capacitive voltage transformer”, International Conference on Applied Superconductivity and Electromagnetic Devices, Beijing, China, Mar. 2014.

[36] I. A. Metwally, “Performance Improvement of Slow-Wave Rogowski Coils for High Impulse Current Measurement”, *IEEE Sensors Journal*, vol. 13, no. 2, pp. 538-547, Feb. 2013.

[37] U. Kumar, “Performance of Rogowski coils at higher frequencies”, International Conference on Lightning Protection, Cagliari, Italy, Feb. 2017.

[38] D. Y. Wang, Z. C. Wang, X. F. Sun, B. C. Wang, “Frequency response analysis of a Rogowski coil transducer for railgun pulse current measurement”, IEEE Pulsed Power Conference, Austin, USA, Oct. 2015.

[39] IEC 61869-10

[40] Uncertainty of measurement, Part 3: Guide to the expression of uncertainty in measurement (GUM:1995)”, ISO/IEC Guide 98-3:2008, International Standardization Organization, Geneva, Switzerland, 2008.

[41] Q. Dou, J. Liu, Z. Liu, T. Liu, “A Novel Online Grid Impedance Measurement Method Based on Injecting Pulses Designed in Frequency-Domain”, IEEE International Power Electronics and Motion Control Conference, Hefei, China, May 2016.